Food Chemistry: X 18 (2023) 100720

Contents lists available at ScienceDirect

Food Chemistry: X

journal homepage: www.sciencedirect.com/journal/food-chemistry-x

Metabolomics revealed metabolite biomarkers of antioxidant properties and flavonoid metabolite accumulation in purple rice after grain filling

Qiangqiang Xiong [a,b], Jiao Zhang [a], Changhui Sun [a], Runnan Wang [a], Haiyan Wei [a,b], Haohua He [c], Dahu Zhou [c,*], Hongcheng Zhang [a,b], Jinyan Zhu [a,b,*]

[a] Jiangsu Key Laboratory of Crop Genetics and Physiology/Jiangsu Key Laboratory of Crop Cultivation and Physiology, Agricultural College of Yangzhou University, Yangzhou 225009, China
[b] Jiangsu Co-Innovation Center for Modern Production Technology of Grain Crops, Yangzhou University, Yangzhou 225009, China
[c] Key Laboratory of Crop Physiology, Ecology and Genetic Breeding, Ministry of Education, College of Agronomy, Jiangxi Agricultural University, Nanchang 330045, China

ARTICLE INFO

Keywords:
Metabolomics
Metabolite biomarker
Flavonoids
Total antioxidant capacity
Purple rice

ABSTRACT

The correlation between flavonoids, phenolic metabolites and the total antioxidant capacity is well established. However, specific biomarkers of metabolites with antioxidant properties in purple rice grains remain unidentified. This study integrated nontargeted metabolomics, quantitative detection of flavonoids and phenolic compounds, and physiological and biochemical data to identify metabolite biomarkers of the antioxidant properties of purple rice grains after filling. The findings demonstrated a significant enhancement in the biosynthesis of flavonoids during the middle and late filling stages in purple rice grains. Additionally, the pathways involved in anthocyanin and flavonoid biosynthesis were significantly enriched. Catalase (CAT), phenylalanine ammonia-lyase (PAL), total phenols (TP), flavonoids (FD), and oligomeric proanthocyanidin (OPC) were significantly correlated with philorizin, myricetin 3-galactoside, and trilobatin. Phlorizin, myricetin 3-galactoside, and trilobatin were metabolite biomarkers of antioxidant properties in purple rice grains. This study provides new ideas for the cultivation of high-quality coloured rice varieties with high antioxidant activity.

Introduction

Rice cultivars with pigments deposited in the caryopsis seed coat represent a unique germplasm resource. These coloured rice cultivars are typically categorized as red rice, green rice, black rice (purple rice), or yellow rice based on the colour of the caryopsis. Among these, red rice and black rice (purple rice) are the most common (Zhao et al., 2022). Purple rice is rich in vitamins, microelements, flavonoids, anthocyanins, and other polyphenols, which have certain functions in health (Zhu et al., 2022a; Xiong et al., 2022a). Free radicals are the intermediate metabolites of many biochemical reactions in human tissues. Typically, the production and removal of free radicals in the human body maintain a dynamic equilibrium. However, any disruption in this equilibrium, whether it is excessive or inadequate production of free radicals, can potentially trigger the onset and development of various diseases (Ito & Lacerta, 2019). Polyphenols present in purple rice are known to exhibit free radical-scavenging and antioxidation functions. These properties enable polyphenols to reduce high fat and cholesterol levels, enhance the antioxidant capacity of the body, and alleviate oxidative damage to various components, including arterial wall cells (Prommachartal et al., 2021; Sirilun et al., 2022). Flavonoids, anthocyanins, and other polyphenols are widely used in health foods, medicines, beauty products, and other products due to their unique antioxidant properties (Yang et al., 2019; Li et al., 2022). Earlier investigations have reported significant improvements in the postprandial blood glucose levels and antioxidant capacity of healthy volunteers upon consumption of purple rice bread (Chusak et al., 2020). Healthy volunteers were administered yogurt containing 0.25% purple rice anthocyanin, leading to a significant decrease in their postprandial glucose levels and a significant enhancement in their plasma antioxidant capacity (Anuyahong et al., 2020). These results highlight the significance of further exploring the mechanism underlying the antioxidant properties of purple rice grains and identifying metabolite biomarkers associated with these properties. The potential for creating health products that use purple rice grains as

* Corresponding authors at: Jiangsu Key Laboratory of Crop Genetics and Physiology/Jiangsu Key Laboratory of Crop Cultivation and Physiology, Agricultural College of Yangzhou University, Yangzhou 225009, China (J. Zhu).
E-mail addresses: zhoudahu2008@163.com (D. Zhou), zhujinyanrain@163.com (J. Zhu).

https://doi.org/10.1016/j.fochx.2023.100720
Received 16 March 2023; Received in revised form 18 May 2023; Accepted 19 May 2023
Available online 24 May 2023

their primary ingredient and may improve human health is significant.

In recent years, databases of metabolic components in rice and other major crops have been established, facilitating systematic investigations into differences in the types and contents of various metabolic components among different crops (Chen et al., 2016; Zhu et al., 2022b; Zhou et al., 2022; Shen et al., 2023). Metabolomics has been widely used to detect various components in plants and plays an important role in the study of plant physiology (Li et al., 2022; Ning et al., 2022). Anthocyanins are natural plant pigments of flavonoids that have strong antioxidant activity and free radical scavenging functions. Therefore, anthocyanins serve crucial physiological purposes, such as reducing inflammation and preventing diabetes and cardiovascular diseases (Yamuangmorn & Prom-u-Thai, 2021). According to research, the colour of the black rice seed coat is determined by two genes, *Pp* and *Pb/Ra1/OsB1*. *Pb/Ra1/OsB1* regulates the presence of seed coat colour, whereas *Pp* determines the intensity of seed coat colour. In the absence of *Pb/Ra1/OsB1*, the seed coat appears white, whereas its presence alone results in a brown seed coat. When both *Pb/Ra1/OsB1* and *Pp* genes are active, the seed coat exhibits a purple hue (Sakamoto et al., 2001; Rahman et al., 2013). In addition, *Kala4/OsB2* encodes a transcription factor containing the bHLH motif, and structural variation in its promoter region leads to a change in its expression. *Kala4/OsB2* determined the characteristics of the black caryopsis of rice by activating the upstream flavonol synthesis gene to produce specific pigments (Oikawa et al., 2015). An earlier study indicated that two types of purple rice grains had comparably greater antioxidant capacities, total proanthocyanidin content, total flavone content, and total phenol content than two types of white rice grains (Xiong et al., 2022b). The nutritional and antioxidant properties of purple rice grains can be significantly affected by processing techniques (Zhu et al., 2022a; Xiong et al., 2023). According to a recent metabolomic study, the levels of flavonoids and phenolic metabolites and the total antioxidant potential of purple rice grains are strongly correlated (Xiong et al., 2022b). However, the antioxidant properties of the metabolite biomarker at different developmental stages after purple rice grain filling are worth further exploration.

In this research, a purple rice variety called Yangzinuo 1 was cultivated independently. The study analysed metabolite accumulation and antioxidant metabolite biomarkers in purple rice grains at different developmental stages after grain filling based on data derived from nontargeted metabolomics, targeted metabolomics, and physiology and biochemistry experiments. Mass spectrometry was used to quantify the metabolite biomarkers that indicate the antioxidant capacity of purple rice grains at different developmental stages after grain filling. The findings of this study offer fundamental data for cultivating new rice varieties with high antioxidant activity and for metabolic engineering.

Material and methods

Plant material and growth conditions

The material under investigation in the current research was Yangzinuo 1 (the full-length growth period of rice is 162 days), a purple rice variety bred independently by the Agricultural College of Yangzhou University. The rice plants were cultivated at the Shatou base of Yangzhou University, in Yangzhou City, Jiangsu Province. The seeds of the rice were planted on May 20, 2022, and the seedlings were raised using blankets. After 25 days of rice seedling growth, the rice seedlings were transplanted. Each hole was planted with 4 rice seedlings, and the row spacing was 30 cm × 12 cm. The rice line planting was carried out with three repetitions. Pure nitrogen was applied at a rate of 300 kg hm^{-2}, and a compound fertilizer containing nitrogen, phosphorus, and potassium in proportions of 15% each was also applied. It was 5:3:2 in favour of basal fertilizer, tillering fertilizer, and panicle initiation fertilizer. Using the requirements for the conventional high-yield cultivation of rice, diseases, pests, and weeds were controlled.

Sample collection

At the heading stage of rice, 300 panicles of the same type, appearance, and size from different rice plants (>2 panicles per plant were taken) were selected in each plot (15 m^2) and labelled. Labelled rice panicles were selected 7 days (Y1G1), 14 days (Y1G2), 21 days (Y1G3), 28 days (Y1G4), and 35 days (Y1G5) after rice filling. The collected rice panicles were transferred back to the laboratory, and tweezers were used to remove the rice shells. The grains were placed in a cryopreservation tube and frozen in liquid nitrogen, and 3 biological replicates were used (each replicate was a mixed sample of 10 rice panicles and grains). The seeds were refrigerated at −20 °C until data collection.

Determination of physiological and biochemical indexes

CAT activity (Johansson & Borg, 1988), polyphenol oxidase (PPO) activity (Park et al., 1997), PAL activity (Aydas et al., 2013), FD content (Ghasemzadeh et al., 2018), OPC content (Chu et al., 2019), TP content (Suleria et al., 2020), and total antioxidant capacity (ABTS method, 2,2′-azino-bis(3-ethylbenzothiazoline-6-sulfonic acid; DPPH method, 2,2-diphenyl-1-picrylhydrazyl; FRAP method, ferric ion reducing antioxidant power method) (Zorzi et al., 2020; Cömert et al., 2020; Abeyrathne et al., 2021) of rice grain samples were determined by instructions provided by Suzhou Michy Biomedical Technology Co., Ltd. (Suzhou Michy Biomedical Technology Co., Ltd. Suzhou, China).

Enzyme activity assay: First, 0.10 g of tissue was weighed, 1 mL of extraction solution was added, and the tissue was homogenized on ice. The solution was centrifuged at 8000 g and 4 °C for 10 min, and the supernatant was collected for further analysis.

Flavonoid assay: The sample was dried to a constant weight, ground and passed through a 40-mesh sieve. A total of 0.05 g of the sample was weighed, and 1 mL of 60% ethanol was added. The mixture was shaken at 60 °C for 2 h and centrifuged at 10,000 g and 25 °C for 10 min. The supernatant was collected for further analysis.

Oligomeric proanthocyanidin assay: First, 0.05 g of the dried sample was weighed, and 1 mL of extraction solution was added. The samples were homogenized and shaken at 60 °C for 2 h and then centrifuged at 10,000 g and 25 °C for 10 min. The supernatant was collected for further analysis.

Total phenol assay: The sample was dried to a constant weight, ground and passed through a 40-mesh sieve. A total of 0.02 g of the sample was weighed, and 1 mL of extraction solution was added. The mixture was shaken at 60 °C for 2 h and centrifuged at 10,000 g and 25 °C for 10 min. The supernatant was collected for further analysis.

ABTS assay: The $ABTS^+$ cation radical is stable and can be dissolved in water or acidic ethanol. It has maximum absorption at 734 nm. The antioxidant components in the sample can react with $ABTS^+$ to cause fading of the reaction system. The change in absorbance at 734 nm was measured, and Trolox was used as a control system to quantify the antioxidant capacity of the sample. A total of 0.10 g of tissue was weighed, and 1 mL of extraction solution was added. The samples were homogenized on ice and then centrifuged at 10,000 g and 4 °C for 10 min. The supernatant was collected for further analysis.

DPPH assay: DPPH is a stable free radical that can be dissolved in polar solvents such as methanol and ethanol. It has maximum absorption at 515 nm. When an antioxidant is added to the DPPH solution, a decolorization reaction occurs. The change in absorbance at 515 nm was measured, and Trolox was used as a control system to quantify the antioxidant capacity of the sample. A total of 0.10 g of the sample was weighed, and 1 mL of extraction solution was added. The samples were homogenized on ice and then centrifuged at 10,000 g and 4 °C for 10 min. The supernatant was collected for further analysis.

FRAP assay: The ability of antioxidants to reduce Fe^{3+}-TPTZ to produce blue Fe^{2+}-TPTZ reflects the total antioxidant capacity. A total of 0.10 g of the sample was weighed, and 1 mL of extraction solution was added. The samples were homogenized on ice and then centrifuged at

10,000 g and 4 °C for 10 min. The supernatant was collected for further analysis.

Sample preparation for metabolite extraction

Fifty milligrams of rice seed sample was placed in a 2 mL centrifuge tube, and a grinding bead with a diameter of 6 mm was added. The sample was extracted using 400 μL of an extraction solution (methanol: water = 4:1 (v: v)) containing 0.02 mg mL^{-1} internal standard (L-2-chlorophenylalanine) to obtain the seed metabolites. The sample was ground for 6 mins at −10 °C and 50 Hz in a frozen tissue grinder before being subjected to a 30-min low-temperature ultrasound extraction process (5 °C and 40 kHz). The extracted material was then kept at −20 °C for 30 mins before being centrifuged for 15 mins. An injection vial with an endotracheal tube was then used to transfer the supernatant for analysis.

Quality control sample

To establish quality control (QC) samples, metabolites from each grain sample were mixed. For every five samples during the instrument analysis, a QC sample was taken to ensure that the analysis process could be repeated.

Ultrahigh-performance liquid chromatography-mass spectrometry (UHPLC-MS/MS) analysis

The Thermo UHPLC system, equipped with an ACQUITY UPLC HSS T3 column (100 mm × 2.1 mm i.d., 1.8 μm; Waters, Milford, USA), was utilized to separate the metabolites.

The mobile phases were composed of 0.1% formic acid in water: acetonitrile (95:5, v/v) (solvent A) and 0.1% formic acid in acetonitrile: isopropanol: water (47.5:47.5:5, v/v) (solvent B). According to the following settings, the solvent gradient changed from 0 to 3.5 min, 0% B to 24.5% B (0.4 mL min^{-1}); from 3.5 to 5 min, 24.5% B to 65% B (0.4 mL min^{-1}); from 5 to 5.5 min, 65% B to 100% B (0.4 mL min^{-1}); from 5.5 to 7.4 min, 100% B to 100% B (0.4 mL min^{-1} to 0.6 mL min^{-1}); from 7.4 to 7.6 min, 100% B to 51.5% B (0.6 mL min^{-1}); from 7.6 to 7.8 min, 51.5% B to 0% B (0.6 mL min^{-1} to 0.5 mL min^{-1}); from 7.8 to 9 min, 0% B to 0% B (0.5 mL min^{-1} to 0.4 mL min^{-1}); and from 9 to 10 min, 0% B to 0% B (0.4 mL min^{-1}). The sample volume injected was 2 μL, and the flow rate was maintained at 0.4 mL min^{-1}. The column temperature was held constant at 40 °C, and all samples were kept at 4 °C throughout the analysis.

The mass spectrometric data were gathered using either a positive or negative ion mode on a Thermo UHPLC-Q Exactive HF-X mass spectrometer with an ESI source. The following adjustments were made to achieve the optimal settings: a heater temperature of 425 °C, a capillary temperature of 325 °C, a sheath gas flow rate of 50 arb, an aux gas flow rate of 13 arb, an ion-spray voltage floating (ISVF) of −3500 V in negative mode and 3500 V in positive mode, and a normalized collision energy of 20–40-60 V rolling for MS/MS. The resolution of the MS/MS was 7500, and the resolution of the full MS was 60000. Data were acquired using the data-dependent acquisition (DDA) mode. The 70–1050 *m/z* detection range was used.

Metabolite statistical analysis

The data were then subjected to peak detection and alignment using Progenesis QI 2.3 (Nonlinear Dynamics, Waters, USA) following the completion of the UPLC-MS analyses. A data matrix containing the peak intensity, retention time (RT), and mass-to-charge ratio (*m/z*) values was created as a result of the preprocessing. Metabolites that appeared in at least 80% of any set of samples were included. By accounting for the accurate mass, the MS/MS fragment spectra, and the isotope ratio difference, reliable biochemical databases such as the Human Metabolome Database (HMDB) (https://www.hmdb.ca/) and the Metlin database (https://metlin.scripps.edu/) were used to identify the mass spectra of these metabolites.

On the Majorbio Cloud Platform (https://cloud.majorbio.com), a multivariate statistical analysis was conducted using the R package ropls (Version 1.6.2, https://bioconductor.org/packages/release/bioc/html/ropls.html) (Ren et al., 2022). Prior to performing the principal component analysis (PCA), the variables related to the metabolites were scaled to unit variances. Prior to performing orthogonal partial least squares-discriminant analysis (OPLS-DA), Pareto scaling was used. To prevent overfitting, model validity was evaluated based on R2 and Q2 values, which offered details on the interpretability and predictability of the model, respectively. In the OPLS-DA model, the variable importance in the projection (VIP) was determined. *P* values were calculated using the single-dimensional paired Student's *t* test. Based on VIP values>1 and *P* values<0.05, differentially expressed metabolites (DMs) were detected. On the Majorbio Cloud Platform (https://cloud.majorbio.com), multivariate statistical analysis was carried out utilizing the ropls R package (Version 1.6.2, https://bioconductor.org/packages/release/bioc/html/ropls.html) from Bioconductor. Based on database searches (https://www.genome.jp/kegg/), the DMs were mapped onto Kyoto Encyclopedia of Genes and Genomes (KEGG) pathways.

Sample pretreatment for quantitative detection of flavonoids and phenols

The standard samples of flavonoids and phenolic compounds were precisely weighed using an analytical balance, and their details are presented in Table S1. The standards were dissolved in methanol to create a stock solution with a concentration of 1 mg mL^{-1}. By diluting this stock solution, working solutions were prepared with different gradients at concentrations of 200 ng mL^{-1}, 80 ng mL^{-1}, 32 ng mL^{-1}, 12.80 ng mL^{-1}, 5.12 ng mL^{-1}, 2.05 ng mL^{-1}, 0.82 ng mL^{-1}, 0.33 ng mL^{-1}, 0.13 ng mL^{-1}, 0.05 ng mL^{-1}, and 0.02 ng mL^{-1}.

Following freeze-drying, 0.0500 g of the sample was introduced into 600 μL of water:methanol (V:V = 1:2, including internal standards succinic acid − 2,2,3,3-d4 and salicylic acid - d4). Then, 400 μL of chloroform was added. Two small steel balls were added, and samples were ground with a grinder (60 Hz, 2 min). After 20 mins of ultrasonic extraction in an ice-water bath, centrifugation at 4 °C and 10,000 g for 10 mins was conducted. Then, 400 μL of supernatant was introduced into a new EP tube. The residue was then added to 400 μL of water: methanol (V:V = 1:2) containing the same abovementioned internal standards. The mixture underwent 20 mins of ultrasonic extraction after being vortexed for 1 min. After centrifuging for 10 min (4 ℃, 13000 rpm), 400 μL of supernatant was added to the previous 400 μL of supernatant to make a total solution of 800 μL. A total of 400 μL of the supernatant was evaporated, and 200 μL of water:methanol (V:V = 18:7) containing the internal standard L-2-chlorophenylalanine was then added. The mixture was redissolved and subjected to a 30 s vortex, two mins of ultrasonication, and a 2 h incubation period at −20 °C. A brown LC injection bottle was used to transfer 200 μL of the supernatant after centrifugation for 10 min at 4 °C and 13000 rpm. This supernatant was then frozen at −80 °C in preparation for analysis. The QC sample was prepared by mixing the extracts of all samples with equal volumes. All extraction reagents were precooled to −20 °C before use.

UPLC-ESI-MS/MS detection

For the purpose of qualitatively and quantitatively detecting target metabolites, UPLC-ESI-MS/MS analysis was employed.

An ultrahigh-performance liquid chromatograph from AB Company (Framingham, Massachusetts, USA) was used as the chromatographic system. To separate phenolic substances, a Waters UPLC HSS T3 (100 × 2.1 mm, 1.8 m) liquid chromatographic column was utilized (Milford, Massachusetts, USA). The following chromatographic conditions were used: injection volume of 5 μL, flow rate of 0.35 mL/min, mobile phase

comprising A (0.1% formic acid water solution) and B (acetonitrile). The gradient elution procedure was set as follows: 0 min A/B (95:5, V/V), 0.8 min A/B (95:5, V/V), 3 min A/B (75:25, V/V), 12 min A/B (56.2:43.8, V/V), 13 min A/B (1:99, V/V), 14.4 min A/B (1:99, V/V), 14.41 min A/B (95:5, V/V), and 15 min A/B (95:5, V/V).

For the mass spectrum conditions, the following settings were employed: Positive ion mode with CUR at 35 psi, EP at 10, IS at 5500, CXP at 10, TEM at 500 ℃, Gas1 at 60 psi, and Gas2 at 50 psi. Negative ion mode with CUR at 35 psi, EP at −10, IS at −4500, CXP at −20, TEM at 500 ℃, Gas1 at 60 psi, and Gas2 at 50 psi. The column temperature was maintained at 40 ℃.

Data analysis of flavonoids and phenols

SCIEX OS-MQ software (American Sciex Company) was used in the current investigation to help with manual inspection and automatically identify and integrate MRM transitions with default values. The total ion current (TIC) (Fig. S1A), extracted negative ion current (Fig. S1B), and extracted positive ion current (Fig. S1C) of each sample had high resolution and a good peak type. The XIC axis of the ion current diagram represented the RT of the metabolite, while the Y-axis represented the ionic strength (cps) of the ion detection. The mass spectrum peaks of each metabolite found in different samples were manually calibrated based on the RT and peak type of the metabolites to assure the precision of the quantitative determination. The relative concentration of each metabolite was represented by the peak area of each chromatographic peak. Based on the associated quantitative mass spectra of standards at various concentrations, the standard curves for various metabolites were produced with the usual concentration value as the abscissa and the region of the mass spectrum peak as the ordinate. The standard curves for various metabolites had a linearity coefficient R2 better than 0.99 (Table S2), showing excellent linearity. Overlapping display analysis (Fig. S1D, E) on the TIC diagram and the analysis of different QC samples indicated high curve overlaps of the TIC diagram of metabolite detection, suggesting good signal stability of the mass spectrometry and liquid system at different time points. The analytical system and method utilized in this investigation were stable, reliable, and appropriate for the quantitative detection of samples because the RSD of each metabolite was<13% (Table S2). For each standard, Table S2 lists the RT, limit of detection and limit of quantification. Finally, the peak area of each sample metabolite was entered into the regression equation fitted by the standard curve to calculate the concentration of each sample metabolite.

The concentration of metabolites was derived based on the sample dilution ratio and other important factors, which ultimately led to the calculation of the absolute concentration associated with every metabolite present in the actual sample. The mathematical formula utilized for the calculations is as follows:

$$\text{Sample metabolite content (ng g}^{-1}) = N1 * N2 * (C * V)/M$$

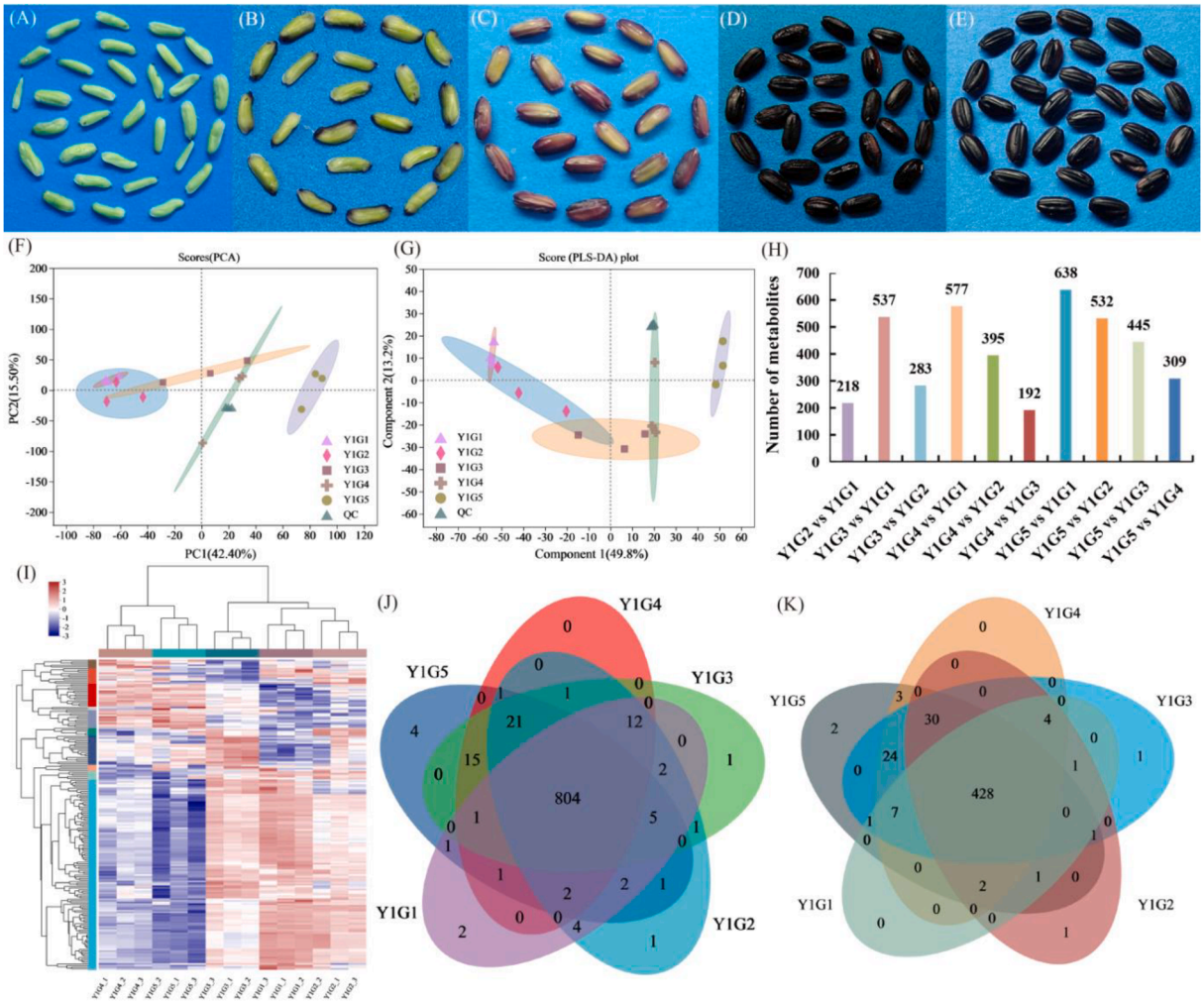

Fig. 1. Grain morphology and metabolite information. (A) 7 days after rice filling (Y1G1); (B) 14 days after rice filling (Y1G2); (C) 21 days after rice filling (Y1G3); (D) 28 days after rice filling (Y1G4); (E) 35 days after rice filling (Y1G5); (F) PCA score; (G) PLS-DA score; (H) DMs of each comparison group; (1) Metabolite clustering thermogram; (J) Venn distribution of metabolites in positive ion mode; (K) Venn distribution of metabolites in negative ion mode.

The formula used to calculate the absolute concentration of metabolites in the actual sample accounts for the dilution ratio and other parameters. In this formula, M stands for the sampling amount (g), N for the conversion factor (10/4), and N2 for the dilution ratio. C represents the concentration value (ng mL-1) determined by estimating the peak area of metabolites in the sample from the standard curve.

Analysis of physiological and biochemical data

The biochemical and physiological data of the grains were sorted, calculated for the average values, and mapped using WPS 2021 software. The statistical analysis of the physiological and biochemical data of the grain samples was performed by carrying out variance analysis (Tukey's test) using SPSS 18.0 software. The graphs were combined using Adobe Illustrator CS6 software.

Results

Metabolic profiling

Differences in the colour of purple rice grains were observed across various developmental stages following grain filling. As time progressed, the grains became darker in colour (Fig. 1A, B, C, D, E). The objective of the investigation was to identify the essential metabolites linked to the antioxidant capacity of purple rice during different developmental phases after grain filling. First, the nontargeted metabolomics of purple rice grains was analysed at five developmental stages after grain filling. The contribution rates of PC1 and PC2 were 42.4% and 15.5%, respectively, with a total contribution rate of 57.9% as per the PCA score chart. The preliminary metabolic difference between samples in each group and the variability between samples in each group were investigated using PCA (Fig. 1F). Additionally, PLS-DA analysis showed that component 1 and component 2 accounted for 49.8% and 13.2% of the variation, respectively (Fig. 1G). This result indicated that the metabolic components of purple rice grains at different developmental stages after grain filling were significantly different. The patterns of metabolite accumulation in purple rice grains at different growth and developmental stages after filling also exhibited differences (Fig. 1I), which is in line with the PCA results.

The study detected a total of 218 DMs between Y1G2 and Y1G1 grains (Fig. 1H; Table S3, Sheet1), with flavonoids representing 1.47% of the total DMs (Table S4). Between Y1G3 and Y1G1 grains, a total of 537 DMs were identified, with flavonoids accounting for 10.53%, isoflavonoids accounting for 1.84%, and phenols accounting for 1.05% (Table S4). Similarly, between Y1G3 and Y1G2 grains, a total of 283 DMs were found (Fig. 1H; Table S3, Sheet3), with flavonoids and phenols accounting for 5% and 2.5% of the total DMs, respectively (Table S4). Between Y1G4 and Y1G1 grains, a total of 577 DMs were detected (Fig. 1H; Table S3, Sheet4), with flavonoids, isoflavonoids, and phenols accounting for 12%, 1.75%, and 0.5% of the total DMs, respectively (Table S4). Between Y1G4 and Y1G2 grains, a total of 395 DMs were identified (Fig. 1H; Table S3, Sheet5), with flavonoids and phenols accounting for 10.37% and 1.11% of the total DMs, respectively (Table S4). Between Y1G4 and Y1G3 grains, a total of 192 DMs were detected (Fig. 1H; Table S3, Sheet 6), with flavonoids accounting for 1.72% of the total DMs (Table S4). Additionally, between Y1G5 and Y1G1 grains, a total of 638 DMs were identified (Fig. 1H; Table S3, Sheet7), with flavonoids and phenols accounting for 11.94% and 1.13% of the total DMs, respectively (Table S4). Between Y1G5 and Y1G2 grains, a total of 532 DMs were found (Fig. 1H; Table S3, Sheet8), with flavonoids and phenols accounting for 11.23% and 1.6% of the total DMs, respectively (Table S4). Between Y1G5 and Y1G3 grains, a total of 445 DMs were detected (Fig. 1H; Table S3, Sheet9), with flavonoids and phenols accounting for 6% and 2% of the total DMs, respectively (Table S4). Finally, between Y1G5 and Y1G4 grains, a total of 309 DMs were identified (Fig. 1H; Table S3, Sheet10), with flavonoids, isoflavonoids, and phenols accounting for 11.06%, 2.3%, and 0.46% of the total DMs, respectively (Table S4).

The Y1G2 and Y1G1, Y1G3 and Y1G2, Y1G4 and Y1G3, and Y1G5 and Y1G4 comparison groups exhibited a relatively small number of DMs (Fig. 1H). The DMs for different comparison groups were visually presented using volcano maps (Fig. S2). The Venn distribution map of metabolites in positive and negative ion modes at different developmental stages of purple rice grains after filling suggested that there may be particular metabolites specific to each stage of grain growth and development. Additionally, more metabolites were observed in positive ion mode than in negative ion mode (Fig. 1J, K).

KEGG analysis

Significant enrichment of differentially accumulated metabolites (DMs) was observed in the starch and sucrose metabolism pathways ($P < 0.05$) between the Y1G2 and Y1G1 comparison groups. The pathways for the biosynthesis of anthocyanins and flavonoids, however, were not significantly enriched ($P > 0.05$; Table 1). The findings revealed that purple rice grains mainly accumulated sugars that constantly enriched the grains at the early filling stage, and there were fewer flavonoids synthesized. Significant enrichment ($P < 0.05$) of DMs in the flavone and flavonol biosynthesis, anthocyanin biosynthesis, and flavonoid biosynthesis pathways was observed when the Y1G3 and Y1G1 groups were compared. On the other hand, the pathways for the metabolism of starch and sucrose were not significantly enhanced ($P > 0.05$; Table 1). This indicated that flavonoid synthesis in purple rice grains increased significantly from 7 to 21 days after grain filling. The Y1G3 and Y1G2 comparison groups did not demonstrate a significant level of DM enrichment in the flavone and flavonol biosynthesis pathways ($P > 0.05$). The phenylpropanoid biosynthesis, anthocyanin biosynthesis, flavone and flavonol biosynthesis, and flavonoid biosynthesis pathways were significantly enriched in DMs derived from the Y1G4 and Y1G1 comparison groups and the Y1G4 and Y1G2 comparison groups. This indicated that flavonoid synthesis in purple rice grains increased significantly from 7 to 28 days and from 14 to 28 days after grain filling. In the Y1G4 and Y1G3 comparison groups, the glyoxylate and dicarboxylate metabolism, citrate cycle (TCA cycle), and glycerophospholipid metabolism pathways were significantly enriched ($P < 0.05$), while the flavone and flavanol biosynthesis pathways did not reach a significant level ($P > 0.05$; Table 1). The Y1G5 and Y1G1 and Y1G5 and Y1G2 comparison groups showed significant enrichment of DMs ($P < 0.05$) in the phenylpropanoid biosynthesis, anthocyanin biosynthesis, flavone and flavonol biosynthesis, and flavonoid biosynthesis pathways. However, the glycolysis/gluconeogenesis, starch, and sucrose metabolism pathways did not exhibit significant enrichment ($P > 0.05$; Table 1). The comparison groups Y1G5 and Y1G4 exhibited significant enrichment ($P < 0.05$; Table 1) of DMs in the anthocyanin biosynthesis, flavone and flavonol biosynthesis, and flavonoid biosynthesis pathways. Sugar accumulation was the main factor in purple rice grains within 14 days of grain filling, and flavonoid synthesis in purple rice grains increased significantly from 14 to 21 days after grain filling. Flavonoid synthesis in purple rice grains increased rapidly when grains were near the mature stage. The comparison group was further analysed with a 14-day interval between grain development after the filling of purple rice. There were 131 DMs between the Y1G3 and Y1G1 comparison groups, the Y1G4 and Y1G1 groups, the Y1G4 and Y1G2 comparison groups, the Y1G5 and Y1G1 comparison groups, the Y1G5 and Y1G2 comparison groups, and the Y1G5 and Y1G3 comparison groups. Among the DMs, phlorizin, trilobatin, epigallocatechin gallate, and myricetin were flavonoid metabolites (Fig. 2A; Table S5).

Physiological and biochemical analyses

The measured enzyme activity, flavonoid content, and total antioxidant capacity of purple rice grains were found to be variable at different

Table 1
KEGG pathways associated with DMs.

Pathway Description[a]	Pathway_ID[b]	Metabolites[c]	*P* value[d]
KEGG pathways enriched in DMs identified between Y1G2 and Y1G1			
Anthocyanin biosynthesis	map00942	C05904	0.2938
Flavonoid biosynthesis	map00941	C05904	0.3231
Starch and sucrose metabolism	map00500	C01083;C00089	0.0156
KEGG pathways enriched in DMs identified between Y1G3 and Y1G1			
Starch and sucrose metabolism	map00500	C01083;C00089	0.1263
Anthocyanin biosynthesis	map00942	C05905;C12140;C05908;C08639	0.0238
Flavone and flavonol biosynthesis	map00944	C10107;C01514;C01750;C01265;C05623	0.0015
Flavonoid biosynthesis	map00941	C10107;C09727;C01709;C01514;C05908;C05905;C01604	0.0002
KEGG pathways enriched in DMs identified between Y1G3 and Y1G2			
Flavone and flavonol biosynthesis	map00944	C05623	0.4034
Fructose and mannose metabolism	map00051	C00392	0.4213
Glyoxylate and dicarboxylate metabolism	map00630	C00417	0.4667
Starch and sucrose metabolism	map00500	C01083;C00089	0.0525
KEGG pathways enriched in DMs identified between Y1G4 and Y1G1			
Pentose and glucuronate interconversions	map00040	C03033	0.6211
Folate biosynthesis	map00790	C00251	0.6211
Pentose phosphate pathway	map00030	C04442;C01236	0.1128
Starch and sucrose metabolism	map00500	C01083;C00089	0.1237
Phenylpropanoid biosynthesis	map00940	C16930;C00482;C05158;C01494	0.0252
Anthocyanin biosynthesis	map00942	C05905;C05904;C12140;C05908;C08639	0.0044
Flavone and flavonol biosynthesis	map00944	C10107;C00389;C01750;C01514;C01265;C05623	0.0002
Flavonoid biosynthesis	map00941	C10107;C09727;C06562;C00389;C05631;C01709;C01514;C05908;C05905;C05904;C01604;C00774	0
KEGG pathways enriched in DMs identified between Y1G4 and Y1G2			
Starch and sucrose metabolism	map00500	C01083;C00089	0.0733
Phenylpropanoid biosynthesis	map00940	C16930;C05158;C12205	0.0485
Anthocyanin biosynthesis	map00942	C05905;C05908;C12140	0.0451
Flavone and flavonol biosynthesis	map00944	C10107;C01514;C00389;C05623	0.0032
Flavonoid biosynthesis	map00941	C10107;C00389;C05631;C01514;C05908;C05905;C01604;C00774	0
KEGG pathways enriched in DMs identified between Y1G4 and Y1G3			
Flavone and flavonol biosynthesis	map00944	C12627	0.2516
Citrate cycle (TCA cycle)	map00020	C00158;C00311	0.0055
Glyoxylate and dicarboxylate metabolism	map00630	C00158;C00311;C00064	0.0048
Glycerophospholipid metabolism	map00564	C00681;C00416;C04230	0.0036
KEGG pathways enriched in DMs identified between Y1G5 and Y1G1			
Glyoxylate and dicarboxylate metabolism	map00630	C00025	0.6729
Starch and sucrose metabolism	map00500	C01083;C00089	0.1394
Phenylpropanoid biosynthesis	map00940	C16930;C02646;C05158;C12205	0.0319
Anthocyanin biosynthesis	map00942	C05905;C05904;C12140;C05908;C08639	0.006
Flavone and flavonol biosynthesis	map00944	C10107;C00389;C01750;C01514;C01265;C05623	0.0002
Flavonoid biosynthesis	map00941	C10107;C09727;C06562;C00389;C05631;C01709;C01514;C05908;C05905;C05904;C01604;C00774	0
KEGG pathways enriched in DMs identified between Y1G5 and Y1G2			
Starch and sucrose metabolism	map00500	C01083;C00089	0.4693
Fructose and mannose metabolism	map00051	C00392	0.604
Glyoxylate and dicarboxylate metabolism	map00630	C00025	0.6551
Pentose and glucuronate interconversions	map00040	C03033	0.6304
Phenylpropanoid biosynthesis	map00940	C16930;C02646;C05158;C12205	0.0273
Anthocyanin biosynthesis	map00942	C05905;C05904;C12140;C05908;C08639	0.0049
Flavone and flavonol biosynthesis	map00944	C10107;C01514;C01265;C00389;C05623	0.0016
Flavonoid biosynthesis	map00941	C10107;C09727;C06562;C00389;C05631;C01514;C05908;C05905;C05904;C01604;C00774	0
KEGG pathways enriched in DMs identified between Y1G5 and Y1G3			
Glycolysis / Gluconeogenesis	map00010	C00031	0.3798
Starch and sucrose metabolism	map00500	C00031	0.4348
Flavone and flavonol biosynthesis	map00944	C10107;C00389;C01265	0.042
Flavonoid biosynthesis	map00941	C10107;C09727;C06562;C00389;C05904;C01604;C00774	0.0001
KEGG pathways enriched in DMs identified between Y1G5 and Y1G4			
Pentose and glucuronate interconversions	map00040	C03033	0.4376
Folate biosynthesis	map00790	C00251	0.4376
Flavone and flavonol biosynthesis	map00944	C10107;C00389;C05623	0.0133
Anthocyanin biosynthesis	map00942	C05904;C05908;C08639	0.0263
Flavonoid biosynthesis	map00941	C10107;C00389;C05631;C05908;C05904;C01604;C00774	0

[a] Pathway description: KEGG pathway name description; [b]Pathway ID: KEGG pathway ID; [c]Metabolites: The KEGG compound IDs corresponding to the metabolites in the pathway that are annotated in the metabolic set. $P < 0.05$ was considered significant enrichment.

developmental stages after filling (Fig. 3). The activities of CAT, PPO, and PAL increased with the growth of purple rice grains towards maturity (Fig. 3A, B, C). The CAT activity exhibited a substantial increase in Y1G5 and Y1G4 compared to Y1G2 and Y1G1 (Fig. 3A). The PPO activity of Y1G5 was significantly higher than that of Y1G4, Y1G3,

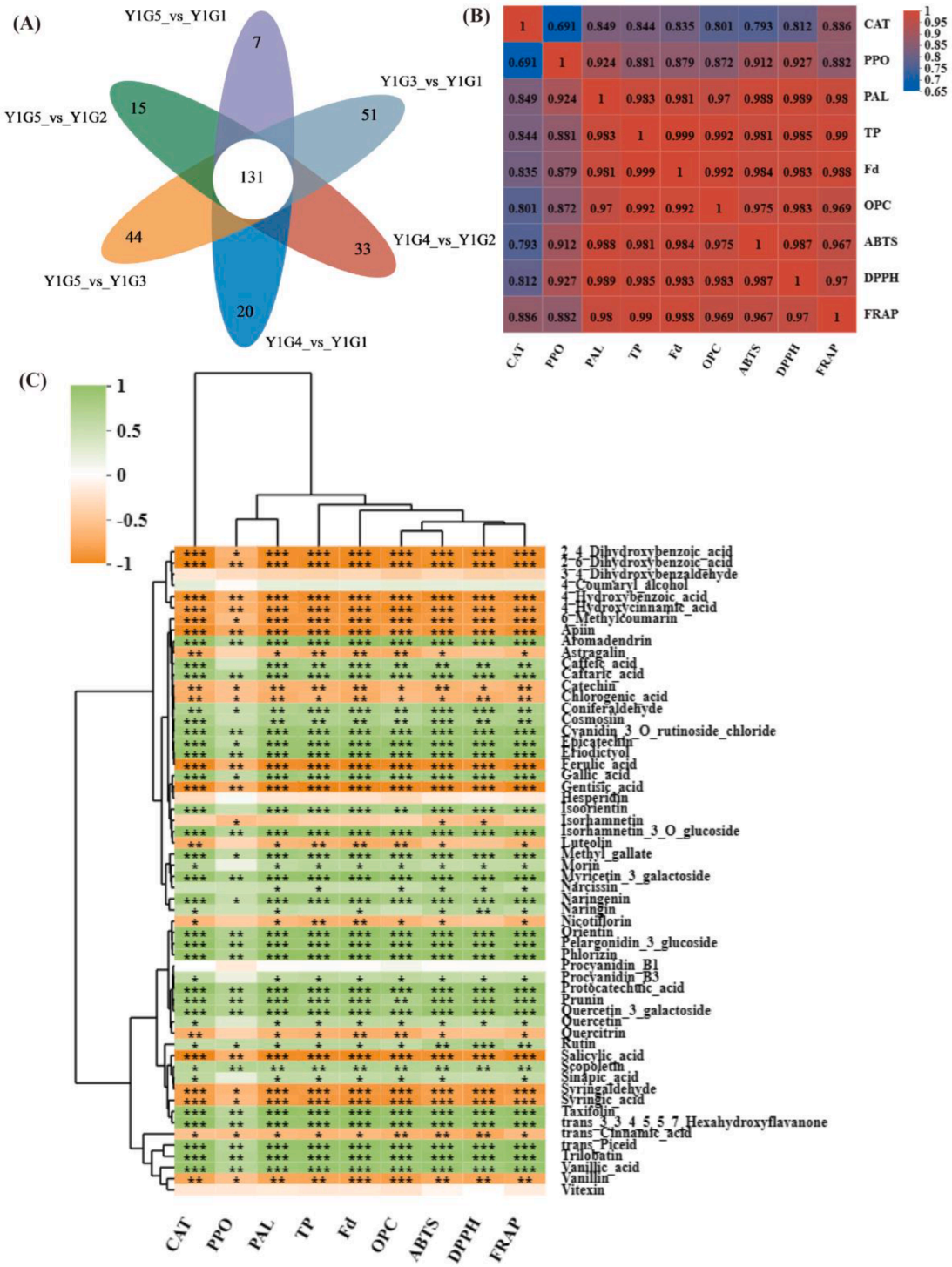

Fig. 2. Venn distribution and correlation analysis. (A) Venn distribution of each comparison group; (B) Correlation analysis of physiological and biochemical indexes; (C) Correlation analysis between physiological and biochemical indexes and flavonoid and phenol content in Table 2. $^{*}P < 0.05$; $^{**}P < 0.01$; $^{***}P < 0.001$.

Y1G2 and Y1G1, specifically, 46.72%, 46.13%, 40.76% and 39.36% higher, respectively (Fig. 3B). Y1G5 exhibited PAL activities that were 234.31% and 221.85% higher than those of Y1G2 and Y1G1, respectively. Meanwhile, Y1G4 showed PAL activities that were 83.03% and 76.21% higher than those of Y1G2 and Y1G1, respectively. Y1G3 exhibited PAL activities that were 37.43% and 32.31% higher than those of Y1G2 and Y1G1, respectively (Fig. 3C). The ABTS method was used to determine the total antioxidant capacity of purple rice grains, and the results showed that Y1G5 and Y1G4 had significantly higher values than Y1G3, Y1G2, and Y1G1 (Fig. 3D). Additionally, the DPPH method was employed to ascertain the total antioxidant capacity of purple rice grains. The DPPH values of Y1G5, Y1G4, and Y1G3 were significantly higher than those of Y1G2 and Y1G1 (Fig. 3E). The FRAP method was employed to measure the total antioxidant capacity of purple rice grains. The DPPH values of Y1G5, Y1G4, and Y1G3 were considerably greater than those of Y1G2 and Y1G1 (Fig. 3F). The three different methods used to ascertain the total antioxidant capacity of purple rice grains showed that Y1G5 had the highest value, whereas Y1G2 and Y1G1 had the

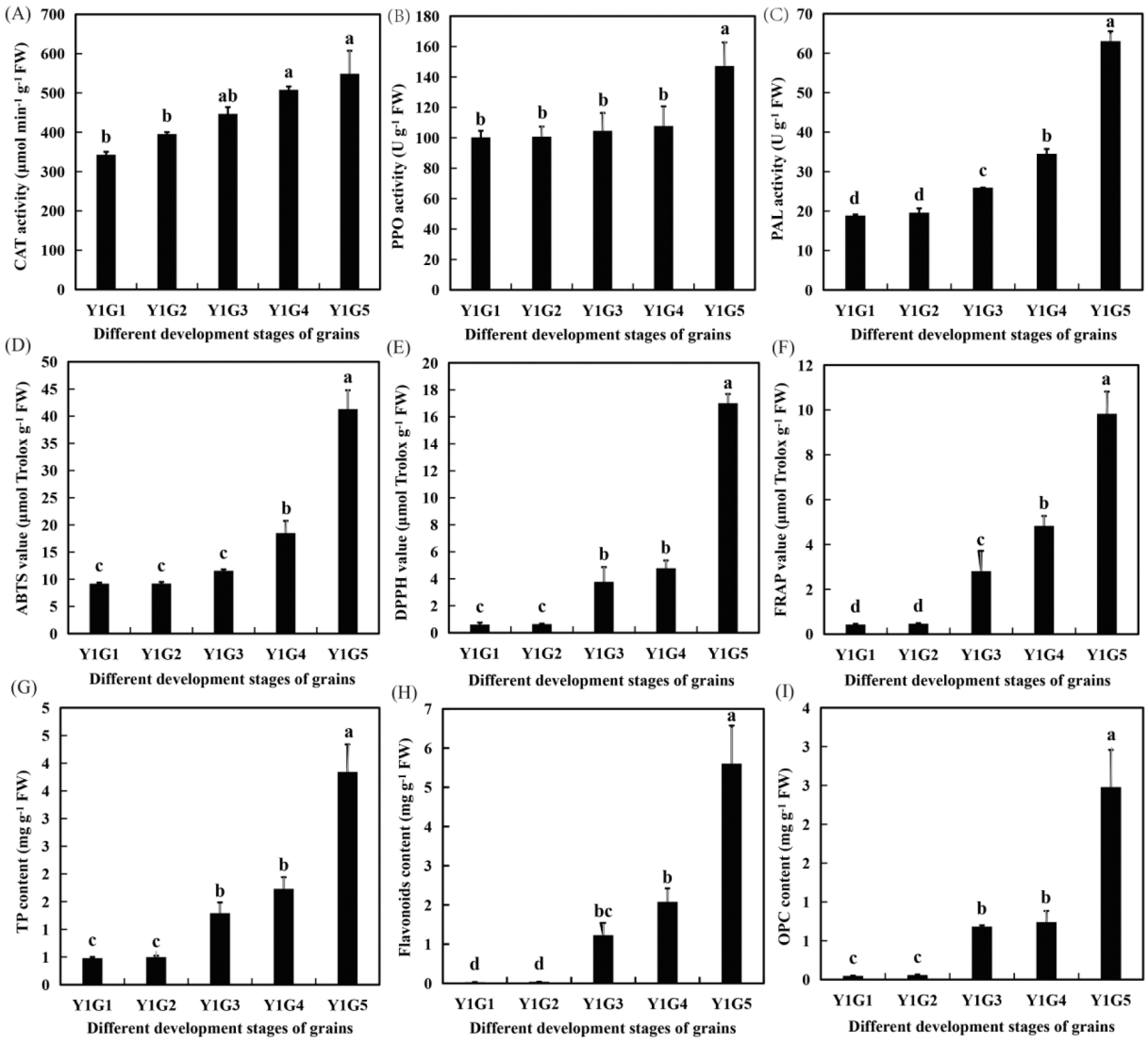

Fig. 3. Analysis of physiological and biochemical indexes of purple rice at different developmental stages after grain filling. (A) CAT activity; (B) PPO activity; (C) PAL activity; (D) ABTS (2,2′-azino-bis(3-ethylbenzothiazoline-6-sulfonic acid) value; (E) DPPH (2,2-diphenyl-1-picrylhydrazyl) value; (F) FRAP (ferric ion reducing antioxidant power) value; (G) TP content; (H) flavonoid content; (I) OPC content. Different lowercase letters represent significance at the 0.05 level.

lowest. Specifically, the ABTS method, DPPH method, and FRAP method all indicated lower total antioxidant capacity in Y1G2 and Y1G1 and higher total antioxidant capacity in Y1G5. The TP content, flavonoid content, and OPC content of Y1G5, Y1G4, and Y1G3 were remarkably higher than those of Y1G2 and Y1G1 (Fig. 3G, H, I). The flavonoid content and OPC content of Y1G2 and Y1G1 were very low (Fig. 3H, I). The correlation analysis of various physiological and biochemical indicators showed that PAL activity, ABTS, DPPH, and FRAP values, and TP, flavonoids, and OPC content were highly correlated, and the correlation coefficients were >0.96 (Fig. 2B). From the overall physiological and biochemical data of different growth and developmental stages of purple rice grains, the longer the interval between grain growth and development, the more significant the differences in antioxidant enzyme activity, total antioxidant capacity, TP content, flavonoid content, and OPC content.

Quantitative analysis of flavonoids and phenolic compounds

A total of 129 flavonoids and phenolic compounds were assessed in this study. Seventy-one flavonoids and phenolic compounds had low or no content (including epigallocathin gallate), so no metabolite level was detected. Therefore, this study quantitatively analysed 58 flavonoids and phenols in different grain developmental stages of purple rice after grain filling (Table 2). The contents of 4-hydroxybenzoic acid, 4-hydroxycinnamic acid, cyanidin 3-O-rutinoside chloride, ferulic acid, salicylic acid, protocatechuic acid, sinapic acid, vanillic acid, and taxifolin in purple rice grains at different developmental stages after grain filling were all high. With the growth and development of purple rice grains towards maturity, the metabolite contents of 2,4-dihydroxybenzoic acid, 6-methylcoumarin, 2,6-dihydroxybenzoic acid, apiin, astragalin, ferulic acid, gentisic acid, luteolin, salicylic acid, and syringic acid were continuously reduced. With the growth and development of purple rice grains towards maturity, the metabolite contents of aromadendrin, caffeic acid, caftaric acid, epicatechin, eriodictyol, cyanidin 3-O-rutinoside chloride, isorhamnetin-3-O-glucoside, myricetin 3-galactoside, orientin, pelargonidin-3-glucoside, phlorizin, protocatechuic acid, prunin, taxifolin, scopoletin, *trans*-3,3′,4′,5,5′,7-hexahydroxyflavanone, *trans*-piceid, trilobatin, and vanillic acid increased. Phlorizin, myricetin 3-galactoside, and trilobatin levels were significantly correlated with CAT and PAL activity, ABTS, DPPH, and FRAP values, and TP, flavonoids, and OPC contents ($P < 0.001$). Phlorizin, myricetin 3-galactoside, and trilobatin levels were significantly correlated with PPO activity ($P <$

Table 2
Quantitative detection of flavonoids and phenolic compounds in purple rice at different developmental stages after grain filling.

Metabolites*	Y1G1	Y1G2	Y1G3	Y1G4	Y1G5
2,4-Dihydroxybenzoic acid	746.24 ± 20.2a	606.11 ± 51.49b	331.24 ± 30.13c	261.48 ± 9.66d	116.03 ± 16.79e
2,6-Dihydroxybenzoic acid	546.88 ± 19.66a	408.18 ± 35.19b	219.54 ± 6.75c	164.80 ± 18.68d	80.26 ± 3.87e
3,4-Dihydroxybenzaldehyde	5.51 ± 0.18a	5.76 ± 0.81a	0.00	6.58 ± 0.88a	0.00
4-Coumaryl alcohol	0.00	0.00	0.28 ± 0.00a	0.15 ± 0.00b	0.00
4-Hydroxybenzoic acid	15740.94 ± 1469.79a	16707.98 ± 350.94a	2739.74 ± 98.46b	1469.82 ± 42.56b	792.08 ± 18.3c
4-Hydroxycinnamic acid	6087.68 ± 54.12a	4782.46 ± 53.82b	2907.18 ± 79.21d	3809.28 ± 97.05c	2482.42 ± 73.06e
6-Methylcoumarin	14.87 ± 1.55a	10.42 ± 0.38b	0.00	0.00	0.00
Apiin	22.52 ± 2.65a	18.57 ± 0.43b	11.88 ± 1.4c	9.32 ± 2.22c	8.76 ± 0.3c
Aromadendrin	5.02 ± 0.52d	8.77 ± 0.85d	15.85 ± 0.12c	46.72 ± 3.08b	51.94 ± 3.99a
Astragalin	4.98 ± 0.66a	0.00	0.00	0.00	0.00
Caffeic acid	0.00	0.00	25.08 ± 1.26a	29.99 ± 4.84a	27.72 ± 5.1a
Caftaric acid	0.00	0.00	0.00	8.49 ± 0.14b	17.93 ± 1.75a
Catechin	1126.06 ± 82.2b	647.94 ± 79.1c	1357.90 ± 109.37a	289.09 ± 24.3d	135.71 ± 7.34e
Chlorogenic acid	9.88 ± 1.28a	8.36 ± 0.78a	9.74 ± 0.38a	0.00	0.00
Coniferaldehyde	2.49 ± 0.29bc	1.42 ± 0.25c	4.08 ± 0.89ab	5.87 ± 1.41a	4.62 ± 0.78a
Cosmosiin	0.00	0.00	0.00	4.82 ± 0.21a	2.78 ± 0.35b
Cyanidin 3-O-rutinoside chloride	1596.78 ± 164.54d	1039.65 ± 185.81d	24970.72 ± 1409.1c	57364.13 ± 5185.77b	85088.92 ± 3679.89a
Epicatechin	0.00	0.00	17.85 ± 3.94b	19.75 ± 7.48b	38.16 ± 2.37a
Eriodictyol	0.13 ± 0.02c	0.58 ± 0.09c	3.82 ± 0.35c	43.02 ± 1.76b	57.02 ± 2.85a
Ferulic acid	13813.62 ± 349.24a	9837.74 ± 704.79b	8786.73 ± 398.01c	8063.12 ± 81.83c	3560.13 ± 31.64d
Gallic acid	12.05 ± 1.24e	21.65 ± 0.17d	59.63 ± 0.96c	91.82 ± 2.47a	72.37 ± 0.94b
Gentisic acid	883.13 ± 25.01a	810.62 ± 12.6b	607.64 ± 27.82c	252.64 ± 9.38d	111.79 ± 4.5e
Hesperidin	665.40 ± 18.81a	78.44 ± 4.86c	48.75 ± 2.61d	77.47 ± 4.19c	136.86 ± 17.61b
Isoorientin	247.38 ± 28.47c	59.91 ± 5.76d	306.96 ± 19.79c	744.72 ± 24.07a	553.47 ± 51.97b
Isorhamnetin	2.01 ± 0.16c	3.49 ± 0.14a	2.89 ± 0.06b	2.24 ± 0.1c	1.47 ± 0.02d
Isorhamnetin-3-O-glucoside	9.74 ± 0.68d	28.85 ± 3.4d	236.47 ± 2.52c	563.49 ± 20.49b	945.73 ± 58.89a
Luteolin	0.48 ± 0.04a	0.00	0.00	0.00	0.00
Methyl gallate	2.74 ± 0.33e	17.34 ± 0.58d	131.71 ± 5.32c	298.39 ± 4.71a	192.46 ± 7.13b
Morin	1.01 ± 0.14d	2.13 ± 0.06c	7.59 ± 0.13a	7.25 ± 0.4a	5.81 ± 0.31b
Myricetin 3-galactoside	2.77 ± 0.19c	33.78 ± 2.55c	594.29 ± 107.4b	717.23 ± 50.55b	1139.31 ± 136.61a
Narcissin	338.40 ± 19.09b	254.83 ± 12.34d	287.56 ± 17.55 cd	330.69 ± 22.23bc	470.89 ± 23.5a
Naringenin	1.77 ± 0.13d	4.06 ± 0.16 cd	5.93 ± 0.37c	24.56 ± 1.98a	12.88 ± 1.8b
Naringin	5.82 ± 1.4c	1.75 ± 0.51c	1.94 ± 0.43c	39.52 ± 7.09a	13.69 ± 2.3b
Nicotiflorin	44.88 ± 4.72a	22.68 ± 2.64c	33.15 ± 0.66b	25.42 ± 2.55c	20.34 ± 0.62c
Orientin	0.00	3.16 ± 0.43c	16.16 ± 1.91c	52.96 ± 2.03b	93.67 ± 18.03a
Pelargonidin-3-glucoside	0.00	11.59 ± 0.46d	337.52 ± 7.22c	1003.37 ± 130.95b	2206.42 ± 68.25a
Phlorizin	1.74 ± 0.16d	7.80 ± 0.68d	34.71 ± 2.35c	72.09 ± 2.89b	183.07 ± 6.37a
Procyanidin B1	0.00	0.00	15.91 ± 1.35a	0.00	0.00
Procyanidin B3	24.12 ± 2.62d	27.10 ± 3.26d	557.80 ± 42.26a	255.52 ± 22.43b	140.70 ± 11.57c
Protocatechuic acid	768.19 ± 4.7d	1155.57 ± 98.78d	3793.91 ± 67.14c	8754.47 ± 216.32b	10909.88 ± 301.76a
Prunin	1.39 ± 0.1c	1.19 ± 0.04c	32.91 ± 3.03b	95.45 ± 13.51a	103.50 ± 8.79a
Quercetin 3-galactoside	78.49 ± 6.54d	0.00	872.68 ± 79.86c	2714.13 ± 152.19b	5719.45 ± 876.73a
Quercetin	1.05 ± 0.07d	2.07 ± 0.2c	8.15 ± 0.56a	7.84 ± 0.32a	5.99 ± 0.04b
Quercitrin	3.28 ± 0.5a	0.00	0.00	0.00	0.00
Rutin	670.19 ± 22.51b	193.18 ± 9.72d	392.99 ± 54.47c	707.55 ± 45.94b	1690.57 ± 35.42a
Salicylic acid	27895.69 ± 128.62a	22325.21 ± 667.32b	13024.91 ± 375.82c	6912.37 ± 238.17d	4407.89 ± 167.18e
Scopoletin	0.00	0.00	0.00	0.00	5.13 ± 0.46a
Sinapic acid	657.97 ± 39.55e	3856.77 ± 141.46d	20923.04 ± 1414.57a	11891.20 ± 950.07b	6979.99 ± 379.06c
Syringaldehyde	128.74 ± 24.6a	83.89 ± 8.09b	54.72 ± 4.76bc	62.46 ± 2.39b	31.01 ± 6.93c
Syringic acid	425.50 ± 66.67a	298.64 ± 11.17b	258.09 ± 25.12b	262.30 ± 44.61b	147.85 ± 20.71c
Taxifolin	491.99 ± 36.54e	1596.30 ± 41.02d	3209.90 ± 130.57c	6716.19 ± 59.93b	8587.87 ± 597.51a
trans-3,3′,4′,5,5′,7-Hexahydroxyflavanone	0.00	0.91 ± 0.18d	8.06 ± 0.72c	53.43 ± 0.78b	207.54 ± 8.6a
trans-Cinnamic acid	529.46 ± 33.81b	919.76 ± 67.24a	322.73 ± 14.02c	552.06 ± 31.99b	91.62 ± 7.19d
trans-Piceid	19.25 ± 1.55d	50.83 ± 3.01d	225.95 ± 20.74c	519.73 ± 35.51b	834.99 ± 83.72a
Trilobatin	0.00	0.00	0.50 ± 0.05c	1.83 ± 0.08b	4.54 ± 0.37a
Vanillic acid	3382.25 ± 263.39d	5812.41 ± 327.52c	7532.26 ± 767.66b	11680.95 ± 1121.67a	11818.33 ± 718.45a
Vanillin	70.45 ± 8.43a	34.81 ± 6.03b	0.00	27.43 ± 1.97b	0.00
Vitexin	378.84 ± 51.5a	96.19 ± 4.45b	96.70 ± 10.58b	131.35 ± 12.6b	120.25 ± 20.97b

*Content of all metabolites, unit: (ng g^{-1}). Different lowercase letters in the same line represent significant differences at the 0.05 level, the same as below.

0.01) (Fig. 2C). Based on these results, it was preliminarily hypothesized that phlorizin, myricetin 3-galactoside, and trilobatin may be metabolite biomarkers for the antioxidant properties of purple rice grains at different growth and developmental stages after grain filling. The higher the content of phlorizin, myricetin 3-galactoside, and trilobatin, the stronger the antioxidation capacity of purple rice grains.

Receiver operating characteristic (ROC) analysis

The study employed ROC analysis to conduct similarity analysis of various sample groups, with the aim of assessing the significance of differences between groups. The area under the curve (AUC) ratios of myricetin, phlorizin, and trilobatin between Y1G2 and Y1G1 were 0.6667, 0.8889, and 0.6667, respectively (Fig. 4A). These findings suggest that the accumulation of antioxidant metabolite biomarkers was insufficient within the first 7 days of grain filling in purple rice, particularly during the early stages of grain development. The AUC ratios of myricetin, phlorizin, and trilobatin between Y1G3 and Y1G1 were 1, 1, and 1, respectively (Fig. 4C). Although the time interval between grain growth and development of purple rice in the Y1G3 and Y1G2 comparison groups was within 7 days after grain filling, the difference in the amount of antioxidant metabolite biomarkers was significant. The AUC ratios of myricetin, phlorizin, and trilobatin between Y1G4 and Y1G1 were 1, 1, and 1, respectively (Fig. 4D). The AUC ratios of myricetin,

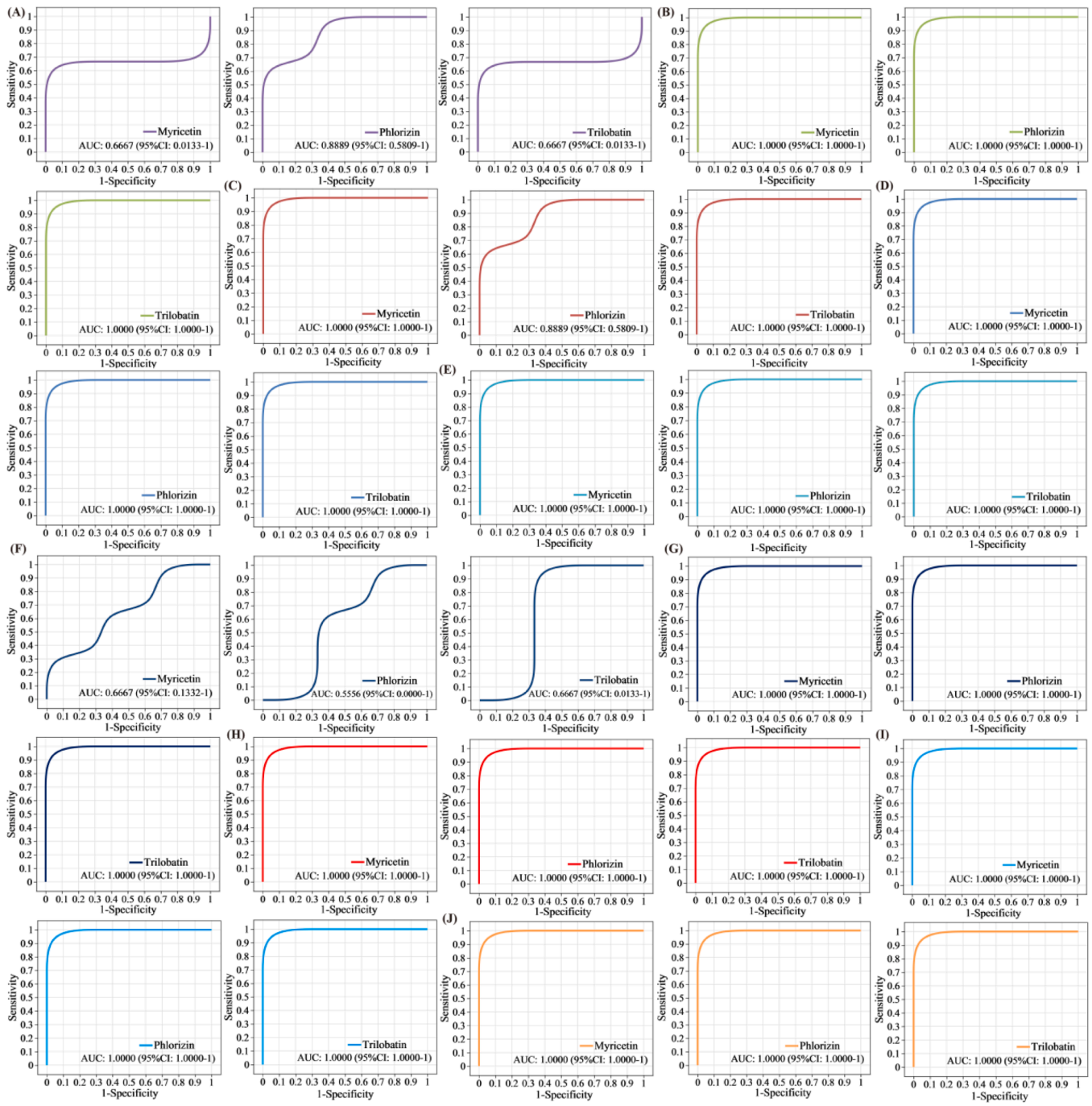

Fig. 4. ROC analysis. (A) ROC analysis of myricetin, phlorizin, trilobatin between Y1G2 and Y1G1; (B) ROC analysis of myricetin, phlorizin, trilobatin between Y1G3 and Y1G1; (C) ROC analysis of myricetin, phlorizin, trilobatin between Y1G3 and Y1G2; (D) ROC analysis of myricetin, phlorizin, trilobatin between Y1G4 and Y1G1; (E) ROC analysis of myricetin, phlorizin, trilobatin between Y1G4 and Y1G2; (F) ROC analysis of myricetin, phlorizin, trilobatin between Y1G4 and Y1G3; (G) ROC analysis of myricetin, phlorizin, trilobatin between Y1G5 and Y1G1; (H) ROC analysis of myricetin, phlorizin, trilobatin between Y1G5 and Y1G2; (I) ROC analysis of myricetin, phlorizin, trilobatin between Y1G5 and Y1G3; (J) ROC analysis of myricetin, phlorizin, trilobatin between Y1G5 and Y1G4. The x-axis is specificity, and the coordinate axis is 1–0. The y-axis is sensitivity, and the coordinate axis is 0–1. The AUC is the area under the corresponding curve. CI represents the 95% confidence interval of the AUC calculated based on the nonparametric resampling method. The point on the curve refers to the best threshold to distinguish the two groups based on the ROC curve.

phlorizin, and trilobatin between Y1G4 and Y1G2 were 1, 1, and 1, respectively (Fig. 4E). The AUC ratios of myricetin, phlorizin, and trilobatin between Y1G4 and Y1G3 were 0.6667, 0.5556 and 0.6667, respectively (Fig. 4F). The accumulation of antioxidant metabolite biomarkers was not sufficient within 7 days of grain filling in purple rice. The AUC ratios of myricetin, phlorizin, and trilobatin between Y1G5 and Y1G1 were 1, 1, and 1, respectively (Fig. 4G). The AUC ratios of myricetin, phlorizin, and trilobatin between Y1G5 and Y1G2 were 1, 1, and 1, respectively (Fig. 4H). The AUC ratios of myricetin, phlorizin, and trilobatin between Y1G5 and Y1G3 were 1, 1, and 1, respectively (Fig. 4I). The AUC ratios of myricetin, phlorizin, and trilobatin between Y1G5 and Y1G4 were 1, 1 and 1, respectively (Fig. 4J). Although the time interval between grain growth and development of purple rice in the Y1G3 and Y1G2 comparison groups was within 7 days of grain

filling, the difference in the amount of antioxidant metabolite biomarkers was significant, and flavonoids rapidly accumulated in grains near maturity. When the AUC ratio > 0.5, the closer the AUC ratio is to 1, the better the diagnostic effect. The accuracy of the AUC ratio is considered low when it falls between 0.5 and 0.7, moderate when it falls between 0.7 and 0.9, and high when it is above 0.9. When the AUC ratio = 0.5, the diagnostic method is ineffective and holds no diagnostic value.

Discussion

Comprehensive analysis of antioxidant metabolites

The green appearance of rice caryopses at the early stage of development is due to the presence of chlorophyll in the pericarp cells; the coloured rice pericarp is the main deposition site of anthocyanins and chlorophyll (Song et al., 2022). In this study, the purple rice grains were mainly green in the early filling stage (Fig. 1A, B). The purple shade of the purple rice grains was obvious at the middle filling stage (Fig. 1C). Previous research has shown that the colour of coloured rice seed coats is related to anthocyanin content and antioxidant capacity. The darker the colour of the coloured rice seed coat, the higher the contents of anthocyanins, flavonoids, and other substances, and the stronger the capacity of antioxidants (Song et al., 2022; Chen et al., 2022). The predominant contributors to the antioxidant activity in 7 varieties of hemp seeds were found to be flavonoids and phenols (Ning et al., 2022). Polyphenols, including hydrolysed tannins, flavonoids, and complex polyphenols, are found at high concentrations in coloured rice. Among polyphenols, flavonoids are one of the important active substances in coloured rice that have antioxidant, antitumour, free radical scavenging, hypoglycaemic, etc., activity (Shao & Bao, 2015; Promachartal et al., 2021; Susanti et al., 2022). Thus, coloured rice with a high polyphenol content is also a raw material that can be used for health product development. The present investigation revealed that the colour of the purple rice grains grew darker as the rice matured (Fig. 1A-E). During the early stage of purple rice grain growth and development, Y1G1 and Y1G2 exhibited significantly lower levels of CAT activity, PAL activity, total antioxidant capacity, TP content, flavonoid content, and OPC content than Y1G4 and Y1G5 in the late stage (Fig. 3A, C-I). The study findings indicated that during the early filling stage of purple rice, the primary factor is sugar accumulation, while the amount of flavonoid synthesis is relatively low. However, with time, after the filling of purple rice, the synthesis of anthocyanins and flavonoid metabolites increases significantly. KEGG pathway analysis revealed that the starch and sucrose metabolism pathways were considerably improved in DMs from the Y1G2 and Y1G1 comparison groups ($P < 0.05$; Table 1). Following the filling of purple rice, the biosynthesis pathways of anthocyanins and flavonoids were remarkably enriched in DMs from various comparison groups after 14 days ($P < 0.05$; Table 1). Plants utilize enzymes such as PAL to synthesize the fundamental structure of anthocyanins from phenylalanine and ultimately produce proanthocyanidins as the final product of the flavonoid metabolic pathway (Zhang et al., 2019; Sharma et al., 2022). The activity of the essential enzyme PAL, which is involved in anthocyanin metabolism, is strongly positively linked to the anthocyanin concentration and flavonoid content of black rice caryopses (Abdel Aal et al., 2006). The results of this study showed a significant association (correlation coefficients > 0.96) between the physiological and biochemical indicators, including PAL activity, ABTS, DPPH, and FRAP values, as well as TP, flavonoid, and OPC content (Fig. 2B). Previous research has demonstrated a strong correlation between the levels of flavonoids and phenolic metabolites and the total antioxidant capacity (Xiong et al., 2022b). In the current study, 131 metabolites were found in the comparison group whose grain development time was 14 days or more after the filling of purple rice. Among the metabolites, phlorizin, trilobatin, epigallocatechin gallate, and myricetin were flavonoid metabolites (Fig. 2A; Table S5). Furthermore, mass spectrometry was used to quantify flavonoids and phenolic compounds in purple rice grains at different growth stages. Phlorizin, myricetin 3-galactoside, and trilobatin levels were significantly highly correlated with CAT, PPO, and PAL activity, ABTS, DPPH, and FRAP levels, and TP, flavonoid, and OPC content ($P < 0.01$; Fig. 2C). As the purple rice grains matured, the levels of phlorizin, myricetin 3-galactoside, and trilobatin metabolites increased (Table 2). Based on these findings, it was hypothesized that phlorizin, myricetin 3-galactoside, and trilobatin could potentially serve as biomarkers for the antioxidant properties of purple rice grains at different stages of growth and development. The higher the contents of phlorizin, myricetin 3-galactoside, and trilobatin were, the stronger the antioxidant activity of the purple rice grains ($P < 0.01$; Fig. 2C). A supervised learning approach was employed to establish linear discrimination and classification models for samples from each group, with the purpose of identifying biomarkers responsible for the abovementioned differences (Cantarino et al., 2019; Carrington et al., 2022).

Validation of antioxidant metabolites

This research further analysed the AUC curves to verify whether the three metabolites were antioxidant metabolite biomarkers at different growth and developmental stages. The accumulation of antioxidant metabolites within 7 days after grain filling in purple rice was not sufficient, especially the accumulation of starch and other carbohydrate substances at the early filling stage. Phenols and flavonoids accumulated rapidly when the purple rice grains were close to maturity. The AUC ratios of the phlorizin, myricetin, and trilobatin metabolites in the Y1G5 and Y1G4 comparison groups were all 1 ($P < 0.01$; Fig. 4J). However, the AUC ratios of the phlorizin, myricetin, and trilobatin metabolites in the six comparison groups (14 days apart) were also all 1 ($P < 0.01$; Fig. 4B, D, E, G, H, I), indicating that phlorizin, myricetin, and trilobatin were very effective antioxidant metabolite biomarkers. Overall, the darker the colour of purple rice grains at different development stages, the higher the content of anthocyanins and flavonoids, and the stronger the antioxidant capacity. It was also found that the metabolite biomarkers of antioxidant properties in different developmental stages were phlorizin, myricetin 3-galactoside, and trilobatin. This study offers an easy-to-use approach for selecting coloured rice varieties in production settings. By focusing on the seed coat colour as the criterion, varieties with darker seed coat colours were identified. Furthermore, the comprehensive antioxidant capacity was utilized as the evaluation parameter to identify superior coloured rice varieties that possess both high anthocyanin content and strong antioxidant activity.

Conclusion

This study employed data from nontargeted metabolomics, flavonoid- and phenol-targeted metabolomics, and physiological and biochemical parameters to identify metabolite biomarkers of antioxidant properties. As time passed after grain filling, the colour of the purple rice grains darkened gradually, and there was an increase in the content of anthocyanins, and flavonoids as well as in the total antioxidant capacity. This study provides a simple method for screening coloured rice varieties with excellent antioxidant properties. Starch and sucrose metabolism were the main characteristics of purple rice grains at the early filling stage. Flavonoids and anthocyanins were mainly synthesized in purple rice after the middle and late filling stages. The higher the content of philorizin, myricetin 3-galactoside, and trilobatin, the stronger the antioxidation capacity of purple rice grains. Phyorizin, myricetin 3-galactoside, and trilobatin are metabolite biomarkers for the antioxidant properties of purple rice grains at different growth and developmental stages after grain filling. The findings of this research can aid in the development of new varieties of coloured rice. Targeted selection of varieties with darker seed coats can be performed to obtain the desired colour. In addition, using the criteria of antioxidant effects,

coloured rice varieties with high antioxidant properties can be identified.

CRediT authorship contribution statement

Qiangqiang Xiong: Investigation, Writing – original draft. **Jiao Zhang:** Data curation. **Changhui Sun:** Investigation, Formal analysis. **Runnan Wang:** Visualization, Investigation. **Haiyan Wei:** Formal analysis. **Haohua He:** Writing – review & editing. **Dahu Zhou:** Writing – review & editing. **Hongcheng Zhang:** Conceptualization, Methodology, Writing – review & editing. **Jinyan Zhu:** Conceptualization, Methodology, Writing – review & editing.

Declaration of Competing Interest

The authors declare that they have no known competing financial interests or personal relationships that could have appeared to influence the work reported in this paper.

Data availability

Data will be made available on request.

Acknowledgements

This work was supported by the Open Project of Key Laboratory of Crop Physiology, Ecology, and Genetic Breeding, Ministry of Education, Jiangxi Agricultural University (202303), Zhenjiang Jinshan Talents Industry Strong City Leading Talent Introduction Plan (Zhenjiang Talent Office [2021] No. 1), Postgraduate Research & Practice Innovation Program of Jiangsu Province (SJCX22_1782), Changzhou Science and Technology Support Plan (Agriculture) (CE20212001), and the Priority Academic Program Development of Jiangsu Higher Education Institutions (PAPD).

Appendix A. Supplementary data

Supplementary data to this article can be found online at https://doi.org/10.1016/j.fochx.2023.100720.

References

Abdel-Aal, E., Young, J., & Rabalski, I. (2006). Anthocyanin composition in black, blue, pink, purple, and red cereal grains. *Journal of Agricultural and Food Chemistry, 54*, 4696–4704.

Abeyrathne, E., Nam, K., & Ahn, D. (2021). Analytical methods for lipid oxidation and antioxidant capacity in food systems. *Antioxidants, 10*, 1587.

Anuyahong, T., Chusak, C., & Adisakwattana, S. (2020). Incorporation of anthocyanin-rich riceberry rice in yogurts: Effect on physicochemical properties, antioxidant activity and in vitro gastrointestinal digestion. *LWT – Food Science and Technology, 129*, Article 109571.

Aydas, S., Ozturk, S., & Aslm, B. (2013). Phenylalanine ammonia lyase (PAL) enzyme activity and antioxidant properties of some cyanobacteria isolates. *Food Chemistry, 136*, 164–169.

Cantarino, I., Carrion, M., Goerlich, F., & Martinez, V. (2019). A ROC analysis-based classification method for landslide susceptibility maps. *Landslides, 16*, 265–282.

Carrington, A., Manuel, D., Fieguth, P., Ramsay, T., Osmani, V., Wernly, B., … Holzinger, A. (2022). Deep ROC analysis and AUC as balanced average accuracy, for improved classifier selection, audit and explanation. *IEEE Transactions on Pattern Analysis and Machine Intelligence, 1*.

Chen, W., Wang, W., Peng, M., Gong, L., Gao, Y., Wan, J., … Luo, J. (2016). Comparative and parallel genome-wide association studies for metabolic and agronomic traits in cereals. *Nature Communications, 7*, 1–10.

Chen, X., Yang, Y., Yang, X., Zhu, G., Lu, X., Jia, F., … Wu, X. (2022). Investigation of flavonoid components and their associated antioxidant capacity in different pigmented rice varieties. *Food Research International, 161*, Article 111726.

Chu, M., Du, Y., Liu, X., Yan, N., Wang, F., & Zhang, Z. (2019). Extraction of proanthocyanidins from Chinese wild rice (*Zizania latifolia*) and analyses of structural composition and potential bioactivities of different fractions. *Molecules, 24*, 1681.

Chusak, C., Pasukamonset, P., Chantarasinlapin, P., & Adisakwattana, S. (2020). Postprandial glycemia, insulinemia, and antioxidant status in healthy subjects after ingestion of bread made from anthocyanin-rich riceberry rice. *Nutrients, 12*, 782.

Cömert, E., Mogol, B., & Gökmen, V. (2020). Relationship between color and antioxidant capacity of fruits and vegetables. *Current Research in Food Science, 2*, 1–10.

Ghasemzadeh, A., Baghdadi, A., Jaafar, Z. E. H., Swamy, M., & Megat Wahab, P. (2018). Optimization of flavonoid extraction from red and brown rice bran and evaluation of the antioxidant properties. *Molecules, 23*, 1863.

Ito, V., & Lacerda, L. (2019). Black rice (*Oryza sativa* L.): A review of its historical aspects, chemical composition, nutritional and functional properties, and applications and processing technologies. *Food Chemistry, 301*, Article 125304.

Johansson, L., & Borg, L. (1988). A spectrophotometric method for determination of catalase activity in small tissue samples. *Analytical Biochemistry, 174*, 331–336.

Li, H., Lv, Q., Liu, A., Wang, J., Sun, X., Deng, J., … Wu, Q. (2022). Comparative metabolomics study of Tartary (*Fagopyrum tataricum* (L.) Gaertn) and common (*Fagopyrum esculentum Moench*) buckwheat seeds. *Food Chemistry, 371*, Article 131125.

Ning, K., Hou, C., Wei, X., Zhou, Y., Zhang, S., Chen, Y., … Chen, S. (2022). Metabolomics analysis revealed the characteristic metabolites of hemp seeds varieties and metabolites responsible for antioxidant properties. *Frontiers in Plant Science, 13*, Article 904163.

Oikawa, T., Maeda, H., Oguchi, T., Yamaguchi, T., Tanabe, N., Ebana, K., … Izawa, T. (2015). The birth of a black rice gene and its local spread by introgression. *The Plant Cell, 27*, 2401–2414.

Park, W., Shelton, D., Peterson, C., Martin, T., Kachman, S., & Wehling, R. (1997). Variation in polyphenol oxidase activity and quality characteristics among hard white wheat and hard red winter wheat samples. *Cereal Chemistry, 74*, 7–11.

Prommachart, R., Uriyapongson, J., Cherdthong, A., & Uriyapongson, S. (2021). Feed Intake, Nutrient Digestibility, Antioxidant Activity in Plasma, and Growth Performance of Male Dairy Cattle Fed Black Rice and Purple Corn Extracted Residue. *Tropical Animal Science Journal, 44*(3), 307–315.

Rahman, M., Lee, K., Lee, E., Matin, M., Lee, D., Yun, J., … Kang, S. (2013). The genetic constitutions of complementary genes Pp and Pb determine the purple color variation in pericarps with cyanidin-3-O-glucoside depositions in black rice. *Journal of Plant Biology, 56*, 24–31.

Ren, Y., Yu, G., Shi, C., Liu, L., Guo, Q., Han, C., Zhang, D., Zhang, L., Liu, B., Gao, H., Zeng, J., Zhou, Y., Qiu, Y., Wei, J., Luo, Y., Zhu, F., Li, X., Wu, Q., Li B., Fu, W., Tong, Y., Meng, J., Fang, Y., Dong, J., Feng, Y., Xie, S., Yang, Q., Yang, H., Wang, Y., Zhang, J., Gu, H., Xuan, H., Zou, G., Luo, C., Huang, L., Yang, B., Dong, Y., Zhao, J., Han, J., Zhang, X., & Huang, H. (2022). Majorbio Cloud: A one-stop, comprehensive bioinformatic platform for multiomics analyses. *iMeta, 1*, e12.

Sakamoto, W., Ohmori, T., Kageyama, K., Miyazaki, C., Saito, A., Murata, M., … Maekawa, M. (2001). The purple leaf (Pl) locus of rice: The Pl w allele has a complex organization and includes two genes encoding basic helix-loop-helix proteins involved in anthocyanin biosynthesis. *Plant and Cell Physiology, 42*, 982–991.

Shao, Y., & Bao, J. (2015). Polyphenols in whole rice grain: Genetic diversity and health benefits. *Food Chemistry, 180*, 86–97.

Sharma, H., Chawla, N., & Dhatt, A. (2022). Role of phenylalanine/tyrosine ammonia lyase and anthocyanidin synthase enzymes for anthocyanin biosynthesis in developing *Solanum melongena* L. genotypes. *Physiologia Plantarum, 174*, e13756.

Shen, S., Zhan, C., Yang, C., Fernie, A., & Luo, J. (2023). Metabolomics-centered mining of plant metabolic diversity and function: Past decade and future perspectives. *Molecular Plant, 16*, 1–21.

Sirilun, S., Chaiyasut, C., Pattananandecha, T., Apichai, S., Sirithunyalug, J., Sirithunyalug, B., & Saenjum, C. (2022). Enhancement of the colorectal chemopreventive and immunization potential of northern Thai purple rice anthocyanin using the biotransformation by β-Glucosidase-Producing *Lactobacillus*. *Antioxidants, 11*, 305.

Song, S., He, A., Zhao, T., Yin, Q., Mu, Y., Wang, Y., … Peng, S. (2022). Effects of shading at different growth stages with various shading intensities on the grain yield and anthocyanin content of colored rice (*Oryza sativa* L.). *Field Crops Research, 283*, Article 108555.

Suleria, H., Barrow, C., & Dunshea, F. (2020). Screening and characterization of phenolic compounds and their antioxidant capacity in different fruit peels. *Foods, 9*, 1206.

Susanti, E., Susilowati, E., & Siswoyo, T. (2022). Effect of germination period on the antioxidant activities and angiotensin-I converting enzyme inhibitory of Indonesian black rice. *Food Research, 6*, 59–67.

Xiong, Q., Zhang, J., Shi, Q., Zhang, Y., Sun, C., Li, A., … Zhu, J. (2022). The key metabolites associated with nutritional components in purple glutinous rice. *Food Research International, 160*, Article 111686.

Xiong, Q., Sun, C., Li, A., Zhang, J., Shi, Q., Zhang, Y., … Zhu, J. (2022). Metabolomics and biochemical analyses revealed metabolites important for the antioxidant properties of purple glutinous rice. *Food Chemistry, 389*, Article 133080.

Xiong, Q., Wang, R., Sun, C., Wang, R., Wang, X., Zhang, Y., … Zhu, J. (2023). Metabolites associated with the main nutrients in two varieties of purple rice processed to polished rice. *Metabolites, 13*, 7.

Yamuangmorn, S., & Prom-u-Thai, C. (2021). The potential of high-anthocyanin purple rice as a functional ingredient in human health. *Antioxidants, 10*, 833.

Yang, W., Kortesniemi, M., Ma, X., Zheng, J., & Yang, B. (2019). Enzymatic acylation of blackcurrant (Ribes nigrum) anthocyanins and evaluation of lipophilic properties and antioxidant capacity of derivatives. *Food Chemistry, 281*, 189–196.

Zhang, Z., Sun, C., Yao, Y., Mao, Z., Sun, G., & Dai, Z. (2019). Red anthocyanins contents and the relationships with phenylalanine ammonia lyase (PAL) activity, soluble sugar and chlorophyll contents in carmine radish (*Raphanus sativus* L.). *Horticultural Science, 46*, 17–25.

Zhao, D., Zhang, C., Li, Q., & Liu, Q. (2022). Genetic control of grain appearance quality in rice. *Biotechnology Advances, 108014*.

Zhou, J., Liu, C., Chen, Q., Liu, L., Niu, S., Chen, R., … Luo, J. (2022). Integration of rhythmic metabolome and transcriptome provides insights into the transmission of

rhythmic fluctuations and temporal diversity of metabolism in rice. *Science China Life Sciences, 65*, 1794–1810.
Zhu, J., Shi, Q., Sun, C., Hu, J., Zhou, N., Wei, H., … Xiong, Q. (2022). Processing affects (decreases or increases) metabolites, flavonoids, black rice pigment, and total antioxidant capacity of purple glutinous rice grains. *Food Chemistry: X, 16*, Article 100492.
Zhu, J., Li, A., Sun, C., Zhang, J., Hu, J., Wang, S., … Xiong, Q. (2022). Rice quality-related metabolites and the regulatory roles of key metabolites in metabolic pathways of high-quality semi-glutinous japonica rice varieties. *Foods, 11*, 3676.
Zorzi, M., Gai, F., Medana, C., Aigotti, R., Morello, S., & Peiretti, P. G. (2020). Bioactive compounds and antioxidant capacity of small berries. *Foods, 9*, 623.